Journal of Thermal Analysis and Calorimetry, Vol. 75 (2004) 13–24

PYROLYSIS STUDY OF SOL–GEL DERIVED TiO_2 POWDERS
Part III. TiO_2-anatase prepared by reacting titanium(IV) isopropoxide with acetic acid

R. Campostrini [1]*, *M. Ischia* [1] *and L. Palmisano* [2]

[1]Dipartimento di Ingegneria dei Materiali, Università di Trento, via Mesiano 77, 38050 Trento, Italy
[2]Dipartimento di Ingegneria Chimica dei Processi e dei Materiali, Università di Palermo, Viale delle Scienze, 90128 Palermo, Italy

(Received March 27, 2003; in revised form September 25, 2003)

Abstract

A homogeneous TiO_2 gel was obtained by hydrolysing titanium(IV) isopropoxide that was previously modified by reaction with acetic acid. The so stabilized precursor was hydrolysed under strong acidic medium (pH=0 by HCl). Dried TiO_2 powders were characterized by FT-IR, XRD, N_2 adsorption analyses, coupled thermogravimetric (TG) gas chromatographic (GC) and mass spectrometric (MS) analyses. A semiquantitative analysis of the main evolved chemical species allowed to depict both the chemical rearrangements occurring in the TiO_2 matrix during pyrolysis and the chemical composition of the initial gel.

Keywords: pyrolysis study, thermogravimetric–mass spectrometric coupled analyses, TiO_2 gel

Introduction

With reference to what reported in the first two parts [1, 2], the results concerning TiO_2 gel obtained by modifying the titanium alkoxide precursor by reaction with acetic acid are presented in this paper. The use of this ligand was presented in previous works [3, 4] but the preparation of this new TiO_2 sample has been carried out by using the same values of the sol–gel parameters employed for samples obtained by reaction with formic and oxalic acids [1, 2]. The reaction of acetic acid with the titanium alkoxide transforms the monomeric tetracoordinate precursor units into oligomeric species. In these oligomers the increase of the coordination sphere of titanium atoms reduces the intrinsic bent of the metal *vs*. hydrolysis reaction, allowing a better control of the gelling process. Moreover, both the precursor modification and the strong acidic medium used in the hydrolysis process lead to a preferential linear growth of the metal–oxide chains yielding a TiO_2 gel structure characterized of a high specific

---

* Author for correspondence: E-mail: renzo.campostrini@ing.unitn.it

1388–6150/2004/ $ 20.00

Akadémiai Kiadó, Budapest
Kluwer Academic Publishers, Dordrecht

surface area. This morphology feature helps the occurrence of a homogeneous polycrystalline TiO_2-anatase phase dispersion, during the subsequent heat treatment, in order to enhance the photocatalytic properties of this material.

The TiO_2 sample presented in this paper was studied in order to compare its thermal stability in respect of other specimens and in particular to confirm the validity of our semi-quantitative TG-MS/TG-GC-MS data processing just in a more intricate case, i.e. when the thermal decomposition of acetate ligands affords the release of several different chemical species. Nevertheless, a precise identification of all the evolved species is required for a correct interpretation of the chemical processes occurring in the rearrangement of the TiO_2 gel matrix. On the other hand, the gas phase elimination of ligand groups, variously coordinated to Ti atoms during gel pyrolysis, generates the formation of new cavity responsible for the microporosity features in the TiO_2 network. Indeed, this fact partially contrasts the densification effect due to the condensation of adjacent not-hydrolyzed groups between Ti–O–Ti chains. Moreover, the increase of degree of freedom of titanium atoms, due to the release of these terminal groups, allows their coordination environmental rearrangement playing a fundamental role in the incipient TiO_2 crystallization into the polymorph phase anatase. For these reasons, the knowledge of the intrinsic pyrolysis mechanisms becomes a crucial aspect in the preparation of polycrystalline TiO_2 anatase powders with tailored morphological features devoted to photocatalytic applications [5–9].

Experimental procedure

Chemicals and instrumentation

Titanium isopropoxide (98.5%) was purchased from ABCR, acetic acid (99.99%), and 2-propanol (99%) were Aldrich reagent grade products. The 1 M hydrochloric acid solution, used to hydrolyse the titanium alkoxide precursor, was obtained diluting a HCl 37% (d=1.186 g cm^{-3}) Carlo-Erba pure reagent grade solution. All chemicals were used as received without any further purification.

The details of instrumentation and analysis procedures concerning sample characterisation by nitrogen adsorption measurements, X-ray diffraction analyses, IR spectroscopy, thermal analyses coupled with mass spectrometric and gas chromatographic measurements are reported in part 1 [1].

Synthesis of sample

0.96 cm^3 of CH_3COOH ($1.67\cdot10^{-2}$ mol) were added dropwise to 4.97 cm^3 of $Ti(OCH(CH_3)_2)_4$ ($1.67\cdot10^{-2}$ mol), previously diluted with 12.8 cm^3 of 2-PrOH (0.167 mol), working under nitrogen flow and the solution was then stirred for 15 min. 0.31 cm^3 of a 1 M HCl solution (corresponding to $1.67\cdot10^{-2}$ mol of H_2O and $3.1\cdot10^{-4}$ mol of H_3O^+), previously diluted in 12.8 cm^3 of 2-propanol (0.167 mol), were added to the modified titanium alkoxide solution yielding a white emulsion. This emulsion, processed in air, turned to a transparent solution yielding a homogeneous gel within 4–5 days. The wet gel was aged in air for one week to obtain a solid, which was milled in a mortar to fine powders. The gel powders were dried at room temperature for 5 days, and then under vacuum (10^{-2} hPa) for further 2 days, yielding the xerogel sample used in the characterization study. Adopted sol–gel parameters were Ti-alkoxide (precursor):acetic acid (ligand):2-propanol (solvent):water:hydrochloric acid (hydrolysis catalyst)=1:1:20:1:0.0184. This titania sample was labelled as TiO_2–Ac.

Results and discussion

Specific surface area and porosity determinations, FTIR and XRD data

An amorphous TiO_2 sample was obtained from the sol–gel synthesis. Polycrystalline TiO_2-anatase powders were recovered by heating the gel at temperatures higher than 400°C, as revealed by XRD spectra, reported in Fig. 1, according to JCPDS card n° 21-1272.

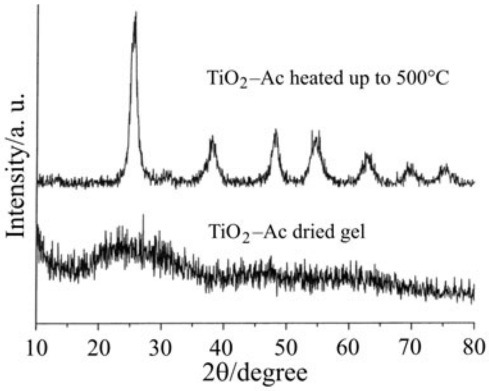

Fig. 1 X-ray diffraction analyses of TiO_2–Ac sample dried at room temperature and after heat treatment up to 500°C

FT-IR spectrum of crude TiO_2 gel shows, together with –O–H and Ti–O–Ti absorptions at 3300 and 600 cm^{-1} [10], two intense bands centred at 1533 and 1450 cm^{-1} due to acetate ligand, variously coordinated to titanium atoms and preferentially bonded in bridging mode by considering the antisymmetric stretching frequency value [3, 4, 11]. These last signals are not present in the annealed samples, as shown in Fig. 2.

N_2 adsorption data, processed by B.E.T. and B.J.H. equations [12, 13], show an isotherm curve typical of a mesoporous material. TiO_2–Ac sample presents specific surface area and average pore diameter of 200 m^2 g^{-1} and 3.4 nm, respectively.

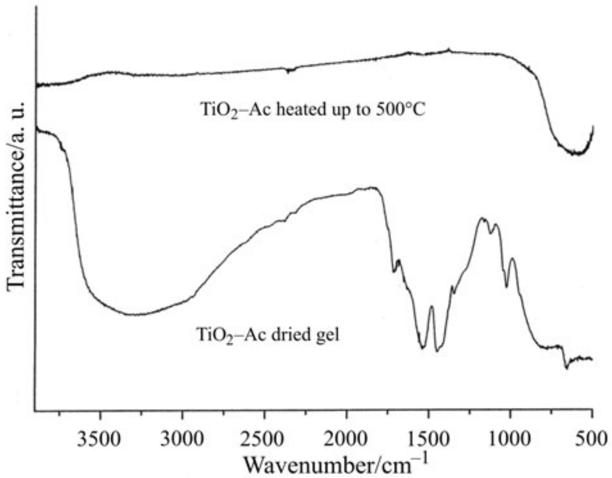

Fig. 2 FT-IR spectra of TiO$_2$–Ac sample dried at room temperature and after heat treatment up to 500°C

Pyrolysis study

Thermogravimetric analysis of TiO$_2$–Ac gel presents a broad mass loss in the 50–450°C range with total intensity of 44.2% as shown in Fig. 3. Derivative TG curve (DTG) shows this event split in two subsequent bands centred at 110 and 340°C, both of them followed

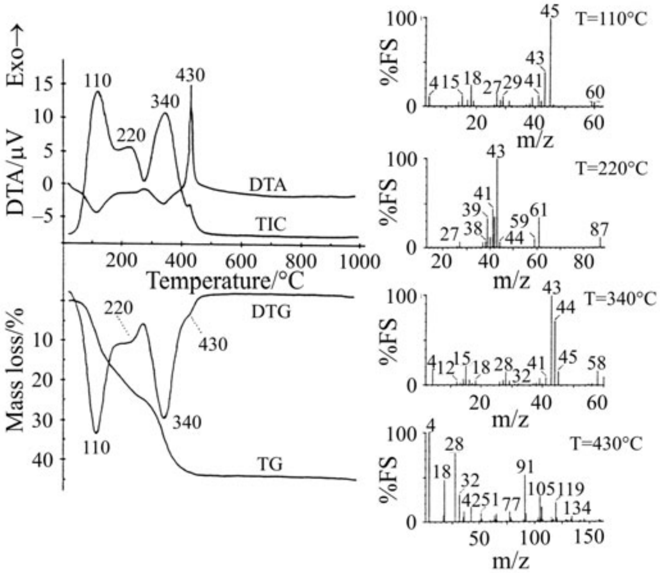

Fig. 3 Thermogravimetric mass spectrometric coupled analyses of TiO$_2$–Ac gel. TG, DTG, DTA curves with the total ion current (*TIC*) plot of the evolved gas phase *vs*. pyrolysis temperature. In the insets mass spectra recorded at the maximum of the *TIC* peaks

by shoulders at 220 and 430°C, respectively. DTA curve presents two endothermic broad bands, according to DTG trend, and a sharp exothermic peak at 430°C (Fig. 3), due to the TiO_2 crystallization [14].

Evolved gas species afforded a total ion current (*TIC*) curve (Fig. 3) which is exactly the symmetric image of DTG trend. Mass spectra recorded inside the first *TIC* peak at 110°C show the evolution of 2-propanol (inset T=110°C, m/z signals at 59, 45) with a minor amount of H_2O (inset T=110°C, m/z 18, 17) and CH_3COOH (inset T=110°C, m/z 60, 43), whereas spectra recorded at 220°C indicate the main release of $CH_3COOCH(CH_3)_2$ (inset T=220°C, m/z 87, 61, 43). H_2O, 2-PrOH and CH_3COOH can derive both from the release of molecules physically adsorbed or entrapped into the TiO_2 network and from thermal promoted condensation reactions involving not hydrolyzed isopropoxide and acetate groups, as observed in previous studies of TiO_2 gels similarly synthesised [3, 4]:

$$\equiv\text{Ti–OH+HO–Ti}\equiv\rightarrow\equiv\text{Ti–O–Ti}\equiv\text{H}_2\text{O}(g) \qquad (1)$$

$$\equiv\text{Ti–OH+(CH}_3)_2\text{CH–O–Ti}\equiv\rightarrow\equiv\text{Ti–O–Ti}\equiv+(\text{CH}_3)_2\text{CHOH}(g) \qquad (2)$$

$$\equiv\text{Ti–OH+CH}_3\text{CO–O–Ti}\equiv\rightarrow\equiv\text{Ti–O–Ti}\equiv+\text{CH}_3\text{COOH}(g) \qquad (3)$$

Isopropyl acetate could arise from gas phase esterification of released acetic acid and 2-propanol, or more probably, by condensation reaction between isopropoxide and acetate groups still coordinated to titanium atoms, as observed by other authors [15].

$$\equiv\text{Ti–OCH(CH}_3)_2+\text{CH}_3\text{COOH}(g)\rightarrow\equiv\text{Ti–OH+CH}_3\text{CO–OCH(CH}_3)_2(g) \qquad (4)$$

$$\equiv\text{Ti–O–COCH}_3+(\text{CH}_3)_2\text{CHOH}(g)\rightarrow\equiv\text{Ti–OH+CH}_3\text{CO–OCH(CH}_3)_2(g) \qquad (5)$$

$$\equiv\text{Ti–OCH(CH}_3)_2+\text{CH}_3\text{CO–O–Ti}\equiv\rightarrow\equiv\text{Ti–O–Ti}\equiv+\text{CH}_3\text{CO–OCH(CH}_3)_2(g) \qquad (6)$$

Some TG-GC-MS analyses were carried out at the maximum intensity of the mass losses in order to characterize the evolved species better by using both OV1 and PoraPlotQ columns. Table 1 summarizes the chemical species detected and identified in these gas chromatograms. Gas samplings at 110°C confirmed the evolution of H_2O, 2-propanol and CH_3COOH, whereas gas chromatograms at 220°C revealed the release of several species, being isopropyl acetate the main component. Actually, other acetic esters were formed and detected, although in very low extent, in a temperature range close to 220°C as summarised in Table 1. The formation of these last compounds required reactions involving structure rearrangements of not-hydrolysed acetate and isopropoxide groups originally bonded to titanium atoms. Propene was also detected around the 200°C temperatures; this olefin arises from elimination reaction of isopropoxide groups:

$$\equiv\text{Ti–OCH(CH}_3)_2\rightarrow\equiv\text{Ti–OH+CH}_3\text{–CH=CH}_2(g) \qquad (7)$$

Moreover, small amounts of 2-chloropropane were also recorded. This chlorinated hydrocarbon could be formed by reaction between released propene and HCl, as previously observed in the thermal behaviour of SiO_2 gels prepared in similar op-

Table 1 Chemical species detected in gas chromatographic elutions (TG-GC-MS analyses) during pyrolysis of TiO_2–Ac sample; 100 mm^3 gas phase sampling

Temp. sampling/ °C	Relative mass loss intensity in the TG curve/%	Capillary column	Identified chemical species[a] (intensity)[b]
110	16.5	Poraplot Q	H_2O(h), 2-PrOH(h), CH_3COOH(l)
		OV1	H_2O(t), 2-PrOH)(h), CH_3COOH(l)
220	8.5	Poraplot Q	H_2O(l), $CH_3CH{=}CH_2$(h), CH_3COCH_3(t), $CH_3CHClCH_3$(t), 2-PrOH(m), CH_3COOH(m), $CH_3COOCH(CH_3)_2$(h)
		OV1	$CH_3CH{=}CH_2$(h), H_2O(l), 2-PrOH(m), CH_3COOH(m), $CH_3COOH(CH_3)_2$(h), $CH_3COO(CH_2)_2CH_3$(l), $CH_3COO(CH_2)_3CH_3$(l)
340	17.8	Poraplot Q	CO_2(h), H_2O(l), $CH_3CH{=}CH_2$(t), one C_4H_8 isomer(m), CH_3COCH_3(h), CH_3COOH(m), $CH_3COOCH(CH_3)_2$(l), $CH_3COO(CH_2)_2CH_3$(l)
		OV1	CO_2(m), one C_4H_8 isomer(m), CH_3COCH_3(h), CH_3COOH(h), one C_7H_{14} isomer(t), one $CH_3COC_4H_7$ isomer(t), $CH_3COCH_2COCH_3$(t), $CH_3COCH{=}C(CH_3)_2$(l), five C_8H_{16} isomers(l), 1,3,5-trimethylbenzene(l), a $CH_3COOC_8H_{17}$ isomer(l)
430	1.4	Porapolot Q	CO(t), CH_4(t), CO_2(h), C_2H_4(t), C_2H_6(t), H_2O(l), $CH_3CH{=}CH_2$(h), C_3H_8(t), $CH_3CHClCH_3$(l), one C_4H_8 isomer(h)+two other C_4H_8 isomers(l), CH_3COCH_3(m), three C_5H_{10} isomers(t), CH_3COOH(l), one C_7H_{12} isomer(t), one C_8H_{16} isomer(m)+five C_8H_{16} isomers(l)
		OV1	CO_2(h), one C_4H_8 isomer(m), CH_3COCH_3(m), un-resolved C_5H_{10} isomers(t), CH_3COOH(m), $CH_3COOCH(CH_3)_2$(t), toluene(t), two dimethylbenzene isomers(l), 1,3,5-trimethylbenzene(m)+two other trimethylbenzene isomers(l), one tetramethylbenzene isomer(t), one $CH_3COOC_8H_{17}$ isomer(t)

[a] Chemical species are listed in order of elution. In the case of isomeric species, attributions were made by comparing their mass spectra with the software data base of the mass spectrometer

[b] The intensity of the eluted species, inside the same gas chromatogram, are approximately evaluated as: *h*=high; *m*=medium; *l*=low; *t*=traces

erative conditions [16]. Actually, hydrochloric acid can derive from the hydrolysis of ≡Ti–Cl bonds, present in low extent inside the TiO_2 gel network, which could be formed during the hydrolysis of Ti-alkoxide precursor occurred under strong acidic catalytic conditions.

From TG-MS analysis during the most intense mass loss, centred at 340°C, mass spectra (Fig. 1) indicate the release of CH_3COCH_3 (inset T=340°C, *m/z* 58, 43) and CO_2 (inset T=340°C, *m/z* 44, 28), with a minor contribution of acetic acid. The first two compounds derive from condensation reaction between two vicinal Ti-acetate groups [3]:

$$2{\equiv}Ti\text{–}O\text{–}COCH_3 \rightarrow {\equiv}Ti\text{–}O\text{–}Ti{\equiv} + CH_3COCH_3(g) + CO_2(g) \tag{8}$$

Mass spectra recorded inside the small shoulder at 430°C show the evolution of CO_2, CO, H_2O and other species with minor intensity (Fig. 3, inset T=430°C).

TG-GC-MS analyses at 340°C confirm the main release, in the same extent, of CH_3COCH_3 and CO_2, and of a butene isomer (probably the 2-methylpropene). Butene isomers could derive from reactions between acetate groups and isopropoxide moieties, yielding in addition CO_2 and H_2, being the last species not well detectable in the operative conditions used:

$$\begin{gathered}{\equiv}Ti\text{–}O\text{–}COCH_3 + (CH_3)_2CH\text{–}O\text{–}Ti{\equiv} \rightarrow \\ {\equiv}Ti\text{–}O\text{–}Ti{\equiv} + CH_2{=}C(CH_3)_2(g) + CO_2(g) + H_2(g)\end{gathered} \tag{9}$$

OV1 chromatogram shows the presence, in very low extent, of some more ‘complex’ organic compounds such as methyl-alkyl-ketone derivatives, unsaturated hydrocarbons (containing up to 8-carbon atoms), and aromatic species like 1,3,5-trimethylbenzene. These high molecular mass compounds could arise from cracking and oligomerization reactions of primary evolved species, occurring on TiO_2 surface. Indeed, TiO_2 matrix could act as heterogeneous catalyst, as observed by other authors [17, 18]. So, for example, detected methyl-benzene derivates can be formed by dehydrogenation and cyclization of propene and butene:

$$CH_3CH{=}CH_2 + (CH_3)_2C{=}CH_2 \rightarrow C_6H_5\text{–}CH_3 + 3H_2 \tag{10}$$

$$2(CH_3)_2C{=}CH_2 \rightarrow C_6H_4\text{–}(CH_3)_2 + 3H_2 \tag{11}$$

$$3CH_3CH{=}CH_2 \rightarrow C_6H_3\text{–}(CH_3)_3 + 3H_2 \tag{12}$$

In the last thermogravimetric event, at 430°C, the presence of these derivatives is further increased as shown in the respective gas chromatographic elutions.

2-Propanol, acetic acid, propene, isopropyl acetate, water, carbon dioxide, acetone and butene were the main compounds constituting the evolved gas mixture, although a wide variety of species was found. The evolution of some of these species during pyrolysis can be easily followed by monitoring the *m/z* ion currents of suitable fragment ions, as shown in Fig. 4, appropriately selected from the mass spectra of the pure substance, as listed in Table 2. 2-Propanol development, followed by *m/z* 45 signal ($[CH_3CHOH]^+$), was centred at 95°C, whereas the two small bands observed at 240 and 300°C were contributions due to fragmentation ions arising from CH_3COOH and

Table 2 Data from mass spectra of pure chemical species and from integrated values of *m/z* ion currents

Chemical species, representative ion [integrated *m/z* value obtained by TG-MS analysis, a. u.]	*m/z* ions from mass spectra of pure substance in TG-GC-MS analyses; (peak height/mm) [integrated *m/z* signal value, a. u.][a]	(Sum of the peak heights/mm) [integrated amount value of the chemical species/a. u.]
H_2O, 18 [$218.61\cdot10^6$]	16(2); 17(19); 18(87)	(108) [$759.18\cdot10^6$]
2-Propanol, 45 [$178.56\cdot10^6$]	15(3); 19(4); 26(2); 27(14); 29(10); 31(6); 37(1); 38(2); 39(6); 40(1); 41(8) [$53.40\cdot10^6$]; 42(4); 43(17); 44(4) [$26.70\cdot10^6$]; 45(87) [$580.77\cdot10^6$]; 46(2); 59(4)	(175) [$1168.22\cdot10^6$]
Propene, 41 [$280.79\cdot10^6$]	15(2); 19(2); 20(1); 25(1); 26(6); 27(21); 36(2); 37(13); 38(18); 39(69); 40(23); 41(87) [$124.31\cdot10^6$]; 42(55); 43(2)	(302) [$431.52\cdot10^6$]
Isopropyl ester, 87 [$25.70\cdot10^6$]	15(4); 27(6); 29(2); 31(2); 39(5); 40(1); 41(13); [$33.42\cdot10^6$]; 42(8); 43(87); 44(3) [$7.71\cdot10^6$]; 45(3) [$7.71\cdot10^6$]; 59(7); 61(16); 87(10)	(167) [$429.26\cdot10^6$]
Acetic acid, 60 [$140.78\cdot10^6$]	13(3); 14(6); 15(16); 16(3); 25(1); 26(1); 28(5); 29(14); 31(5); 40(1); 41(4) [$10.06\cdot10^6$]; 42(14); 43(87); 44(5); [$12.57\cdot10^6$]; 45(78) [$196.08\cdot10^6$]; 46(2); 60(56); 61(1)	(302) [$759.18\cdot10^6$]
Butene, 56 [$26.93\cdot10^6$]	15(1); 26(3); 27(13); 28(13); 29(8); 37(4); 38(7); 39(48); 40(11); 41(87) [$52.06\cdot10^6$]; 42(3); 49(2); 50(6); 51(5); 52(1); 53(6); 54(2); 55(19); 56(45); 57(3)	(287) [$171.74\cdot10^6$]
CO_2, 44 [$490.47\cdot10^6$]	12(2); 16(4); 28(5); 44(87) [$438.46\cdot10^6$]; 45(1)	(99) [$498.93\cdot10^6$]
Acetone, 58 [$85.48\cdot10^6$]	14(3); 15(17); 26(2); 27(4); 29(2); 37(2); 38(3); 39(4); 40(1); 41(3) [$7.54\cdot10^6$]; 42(8); 43(87); 44(2) [$5.03\cdot10^6$]; 58(34); 59(2)	(174) [$437.47\cdot10^6$]

[a] For the sake of conciseness, only the values used in the processing data are summarized

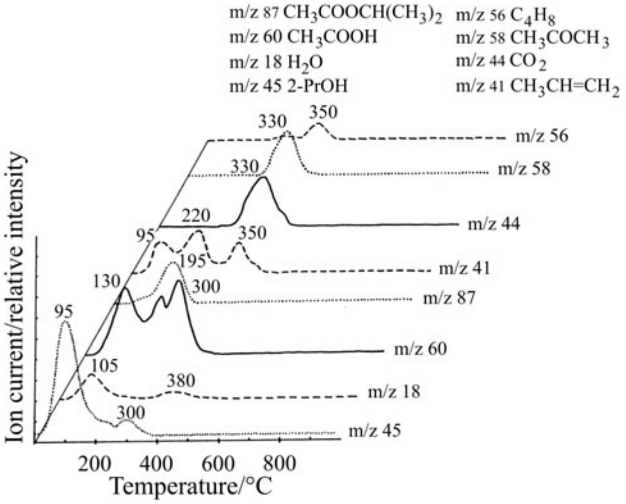

Fig. 4 Ion currents of selected ions chosen to represent the main released chemical species during TiO_2–Ac gel pyrolysis. The intensity of each *m/z* ion current is plotted considering the molar concentration value found for that compound in the TG-MS semiquantitative analysis (Table 3)

CO_2 release. The pyrolysis temperature increase leaded to a main H_2O evolution (*m/z* 18) ($[H_2O]^{+\bullet}$) at 105°C, followed by a less intense one at 380°C. The acetic acid release (*m/z* 60) ($[CH_3COOH]^{+\bullet}$) was also observed in two events, of similar intensity, at 130 and 300°C, with a third smaller one at 240°C. Isopropyl acetate (*m/z* 87) ($[CH_3COOCHCH_3]^+$) development was detected at 195°C. The release of this ester together with the propene one gave rise to the formation of the shoulder at 220°C in the *TIC* curve. *M/Z* 41 ion current, used to monitor propene release ($[CH_2CHCH_2]^+$), showed three subsequent bands at 95, 220 and 350°C. Indeed, the first event was due to an ion arising from the fragmentation of 2-propanol and the last one to the evolution of butene. Both *m/z* 44 and 58 ion currents, attributed to CO_2 ($[CO_2]^{+\bullet}$) and acetone ($[CH_3COCH_3]^{+\bullet}$) formation, respectively, presented the same trend characterized by a single broad band centred at 330°C. Finally, butene release was detected, by means of *m/z* 56 signal ($[C_4H_8]^{+\bullet}$), in a temperature range around 350°C together with the formation of the compounds with higher molecular mass.

The trend of the global release of all compounds can be obtained by considering the sum of the ions currents used to monitor the single species. This last curve was perfectly overlapped to that representing the total ion current, as shown in Fig. 5. This fact confirms the reliability of the proposed interpretation of the pyrolysis mechanism.

A semiquantitative evaluation of pyrolysis data

Thermogravimetric analysis of TiO_2–Ac gel was carried out on 56.9 mg of sample yielding a residual solid of 31.7 and 25.2 mg of evolved gas. The amounts of the main detected species constituting the released gas mixture, i.e. 2-propanol, water,

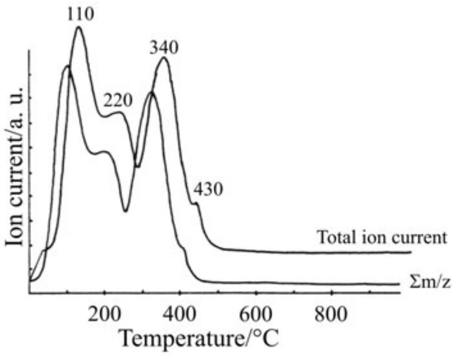

Fig. 5 Comparison between the experimental total ion current curve (*TIC*) with the trend of the curve obtained adding the signals of the *m/z* ion currents chosen to represent the main evolved species in TiO_2–Ac gel pyrolysis

propene, carbon dioxide, acetone, acetic acid, butene and isopropyl ester, were calculated from TG-MS data as described in part 1 [1]. The relative intensities of all ions ($r(i)_j=h(i)_j/\ h(i)_j$), detected in the mass spectrum of each chemical species (j), with their integrated *m/z* ion current values ($Im/z(i)$) for those ions used in data processing, are reported in Table 2.

Butene, acetic acid, water, acetone and isopropyl acetate amounts ($A(j)=Im/z(i)/r(i)$) were first directly evaluated considering the integrated signal ($Im/z(i)_j=Im/z(i)_{\text{TG-MSdata}}$) of their representative ions (respectively *m/z* 56, 60, 18, 58 and 87), being these ions exclusively formed from the ionization and fragmentation process of that compound only. 2-Propanol amount was then calculated from the integrated value of *m/z* 45 signal, neglecting the contribute due to CO_2 release which occurs in another temperature range, and subtracting the contribution of CH_3COOH and $CH_3COOCH(CH_3)_2$ species:

$$Im/z(45)_{\text{2-propanol}}=Im/z(45)_{\text{TG-MSdata}}–Im/z(45)_{\text{acetic acid}}–Im/z(45)_{\text{isopropyl acetate}}=$$

$$=784.56\cdot10^6–196.08\cdot10^6–7.71\cdot10^6=580.77\cdot10^6.$$

Released CO_2 amount was determined from the integrated signal of 44 *m/z* ion current subtracting the contribution of 2-PrOH, CH_3COOH, CH_3COCH_3 and $CH_3COOCH(CH_3)_2$:

$$Im/z(44)_{\text{carbon dioxide}}=$$

$$=Im/z(44)_{\text{TG-MSdata}}–Im/z(44)_{\text{2-propanol}}–Im/z(44)_{\text{acetic acid}}–$$

$$–Im/z(44)_{\text{acetone}}–Im/z(44)_{\text{isopropyl acetate}}=$$

$$=490.47\cdot10^6–26.70\cdot10^6–12.57\cdot10^6–5.03\cdot10^6–7.71\cdot10^6=438.46\cdot10^6.$$

Finally, the amount of propene was evaluated from *m/z* 41 signal considering the co-presence of 2-PrOH, CH_3COOH, C_4H_8, CH_3COCH_3 and $CH_3COOCH(CH_3)_2$:

$$Im/z(41)_{\text{propene}}=$$
$$=Im/z(41)_{\text{TG-MSdata}}-Im/z(41)_{\text{2-propanol}}-Im/z(41)_{\text{acetic acid}}-Im/z(41)_{\text{butene}}$$
$$-Im/z(41)_{\text{acetone}}-Im/z(41)_{\text{isopropyl acetate}}=$$

$$=280.79\cdot10^6-53.40\cdot10^6-10.06\cdot10^6-52.06\cdot10^6-7.5410^6-33.42\cdot10^6=124.31\cdot10^6.$$

Subsequently, the absolute amount of each released species during the entire pyrolysis process has been determined from data of Tables 2 and 3, which show the chemical composition of the evolved gas phase and the intensity of the sample mass loss. The 'degree of identification' of the gas mixture (i.e. $\Sigma A(j)/I_{\text{TIC}}=4167.70\cdot10^6/4979.55\cdot10^6$) was 84%.

Table 3 Chemical composition of gas mixture (25.2 mg) evolved in the whole TiO$_2$–Ac pyrolysis process calculated from TG-MS data

Chemical species (molecular mass)	Molar%	Mass%	Amount/mmol
CO$_2$ (44)	10.7	8.8	$5.04\cdot 10^{-2}$
H$_2$O (18)	16.3	5.5	$7.70\cdot 10^{-2}$
2-Propanol (60)	25.1	28.3	$11.88\cdot 10^{-2}$
Propene (42)	9.3	7.3	$4.38\cdot 10^{-2}$
Isopropyl acetate (102)	9.2	17.6	$4.35\cdot 10^{-2}$
Acetic acid (60)	16.3	18.4	$7.72\cdot 10^{-2}$
Butene (56)	3.7	3.9	$1.76\cdot 10^{-2}$
Acetone (58)	9.4	10.2	$4.43\cdot 10^{-2}$

The amounts of isopropoxide, hydroxyl and acetate groups originally bonded to the titanium atoms (0.3967 mmol) inside the TiO$_2$ network, 0.2237, 0.3062 and 0.2269 mmol, respectively, were then calculated by taking into account the proposed pyrolysis mechanism described by Eqs (1)–(9). So, 0.8302 mmol of bridging oxygen bonds, which correspond to 0.4151 mmol of oxygen atoms, were calculated from the difference between the 1.587 mmol of titanium atom bonds and the 0.7569 mmol of bonds with the above terminal groups.

This gel composition, nominally $TiO_{1.05}(OH)_{0.77}(OCH(CH_3)_2)_{0.56}(OCOCH_3)_{0.57}$, leads to a mass balance of 57.4 mg of crude TiO$_2$ sample in comparison with the experimental 56.9 mg leading to a relative error of +0.9%.

Conclusions

The hydrolysis of the acetate-modified Ti alkoxide precursor, carried out under strong acidic catalytic conditions, allowed to prepare an amorphous titania gel of high specific surface area. A complete crystallization to anatase phase was observed by heating this TiO$_2$ powders at 430°C. In spite of the numerous different species detected by TG-GC-MS measurements, the main processes occurring during pyrolysis are: the condensation reactions, which release molecules of H_2O and 2-propanol; the hydrolysis of the ligand, with development of CH_3COOH; the thermal decomposition of isopropoxide groups with the elimination of propene. The particular reactivity of the acetate group enriches the evolved gas mixture with several other compounds, arising from the decomposition reactions involving the interaction between vicinal acetate and/or isopropoxide groups. These reactions required methyl migration and decarboxylation, yielding relevant amounts of CO_2, acetone and butene, beside the release of isopropyl acetate. Nevertheless, the articulate pyrolysis process and the correct recognition of the main reactions occurring during TiO_2 network rearrangement are confirmed by the quite good results regarding the mass balance of the initial TiO_2 gel. This TG-MS data elaboration allows also to describe the chemical composition of the TiO_2 matrix from the semiquantitative analysis of the evolved gas phase.

References

1 R. Campostrini, M. Ischia and L. Palmisano, J. Therm. Anal. Cal., 71 (2003) 997.
2 R. Campostrini, M. Ischia and L. Palmisano, J. Therm. Anal. Cal., 71 (2003) 1011.
3 G. Marcì, L. Palmisano, A. Sclafani, A. M. Venezia, R. Campostrini, G. Carturan, C. Martin, V. Rives and G. Solana, J. Chem. Soc., Faraday Trans., 92 (1996) 819.
4 G. Facchin, G. Carturan, R. Campostrini, S. Gialanella, L. Lutterotti, L. Armelao, G. Marcì, L. Palmisano and A. Sclafani, J. Sol–Gel Sci. Techn., 18 (2000) 29.
5 A. Sclafani, L. Palmisano and M. Schiavello, J. Phys. Chem., 94 (1990) 829.
6 G. C. Bond, S. Flamerz and L. van Wijk, Catal. Today, 1 (1987) 229.
7 S. S. Chan, I. E. Wachs, L. L. Murrel, L. Wang and W. K. Hall, J. Phys. Chem., 88 (1991) 5831.
8 M. A. Vuurman, I. E. Wachs and A. M. Hirt, J. Phys. Chem., 95 (1991) 9928.
9 G. Ramis, G. Busca, C. Cristiani, L. Lietti, P. Forzatti and F. Bregani, Langmuir, 8 (1992) 1744.
10 T. Lopez, E. Sanchez, P. Bosch, Y. Meas and R. Gomez, Mater. Chem. Phys., 32 (1992) 141.
11 K. Nakamoto, Infrared and Raman Spectra of Inorganic and Coordination Compounds, Wiley, New York 1986.
12 S. J. Gregg and K. S. W. Sing, Adsorption, Surface Area and Porosity, Academic Press, London 1982.
13 P. A. Webb and C. Orr, Analytical Methods in Fine Particles Technology, Ed. Micromeritics Instrument Corporation, Norcross, USA 1997.
14 B. D. Stojanovic, Z. V. Marinkovic, G. O. Brankovic and E. Fidancevska, J. Therm. Anal. Cal., 60 (2000) 595.
15 D. P. Birnie III, J. Mater. Sci., 35 (2000) 367.
16 R. Campostrini, M. Ischia, G. Carturan, S. Gialanella and L. Armelao, J. Sol–Gel Sci. Techn., 18 (2000) 61.
17 K. S. Kim and M. A. Barteau, J. Catal., 125 (1990) 353.
18 H. Idriss, K. S. Kim and M. A. Barteau, J. Catal., 139 (1993) 119.